Analytical vs Experimental Determination of Thermal Resistance with Scalable DC HEMT Model

Sagar Karalkar and Kanti Prasad
Electrical & Computer Engineering
University of Massachusetts Lowell
Lowell, MA 01854, USA

Yu Zhu, Jerod Mason, and Dylan Bartle
Skyworks Solutions Inc.
Woburn, MA 01801, USA

Abstract **–This paper presents a new approach for extracting thermal resistance analytically and comparing it with experimental data along with scalable DC HEMT models for devices with varying Nf and Ugw. Analytical approach to predict the devices temperature increase distribution and calculate the thermal resistance with the help of that is shown. Temperature profile across the fingers with varying devices is carried out and compared with the experimental data. In this way, the analytical values for thermal resistance obtained with the temperature distribution and thermal values used for fitting the output, transfer characteristics are very close to each other and a very good fitting of each device have been achieved.**

Index terms **– HEMTs, thermal resistance, optimization, tuning, circuit simulation, equivalent circuit, semiconductor device modeling and switching application**

I. INTRODUCTION

The thermal property of solid state devices has been very important in designing of the circuit. GaAs IC suffer even more from thermal effects since the thermal conductivity of GaAs is very less to that of silicon. HEMT is widely used in monolithic microwave integrated circuit (MMIC). In order to achieve the best circuit performance, device size needs to be optimized. An accurate scaling model will allow circuit designers to get the desired performance by choosing the right size devices. With the increase in the power density of semiconductor devices, a scalable model with scalable thermal resistance becomes critical for predicting the thermal performance of different sized devices in a broad, dynamic operating range. [1]-[3].

Many techniques have been reported for measuring the thermal resistance of the devices, which are IRM [4], and pulsed electrical method [5]-[7], liquid crystal thermography for determining the hot spot [8] and dc electrical method which is used for measuring the thermal resistance using temperature dependence of gate metal resistivity [9].

In this paper, a novel approach is proposed for determination of thermal resistance by analytical approach and comparing it with the experimental data. The temperature increase is analytically solved with the rectangular heat source and the compared the experimental temperature increase of each device. The temperature behavior is seen across each finger of the device. The thermal resistance value used to fit the output and transfer characteristics of all the devices are compared with the analytical approach.

IJERT

II.EXPERIMENT

Pseudomorphic AlGaAs/InGaAs/GaAs HEMT with ground-signal-ground test pads were fabricated on semi insulating GaAs substrates. The temperature increase of each device were measured with the help of QFI thermal imaging..The transfer and output performances were measured via probe station. Ten devices with different geometry were measured and the data was recorded for individual devices. The ten devices with different geometries are shown below in Table I.

Nf	Ugw(μm)	Total Gate Width
5	143	.715mm
7	143	1mm
14	143	2mm
21	143	3mm
24	143	3.4mm
5	25	.125mm
5	50	.25mm
5	75	.375mm
5	100	.5mm
5	200	1mm

TABLE I: Device Geometry

(This work is licensed under a Creative Commons Attribution 4.0 International License.)

In table I, Nf is the number of fingers and Ugw is the unit gate width. Five devices with Varying Nf and other five devices with varying Ugw are shown above. The output performance was measured in the bias range of Vg = -1 to 0V and Vd = 0 to 3 V, transfer performance was measured in the range of Vd = 1 to 3 V and Vg = -1 to 0.5V and Ig -Vg (diode output) was measured in the range of Vg -3 to 1.2V with Vd constant. The device self-heating measurement of each device was carried from 1 to 3V.

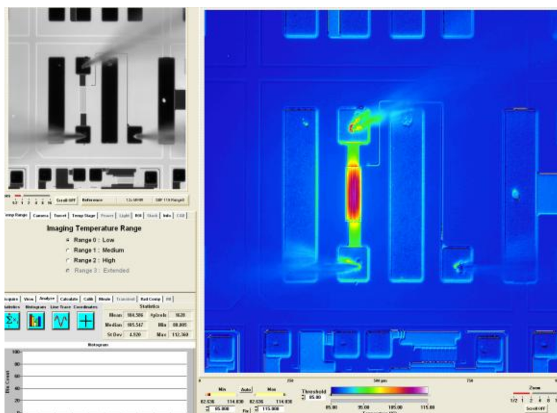

Fig 1: Device 1mm (Varying Nf)

Device (mm)	Voltage (V)	Power (W)	Temp measured Value (^{0}C)
0.715	1	0.1	89.8
0.715	2	0.28	97.3
0.715	3	0.36	127
1	1	0.12	90.16
1	2	0.34	112.3
1	3	0.45	133.1
2	1	0.15	91.5
2	2	0.48	114.1
2	3	0.69	152.4
3	1	0.19	92.45
3	2	0.72	120.8
3	3	1.02	176.1
3.4	1	0.23	95.89
3.4	2	0.86	126.8
3.4	3	1.23	184.3

TABLE II: Measured Temperature
(Devices with Varying Nf)

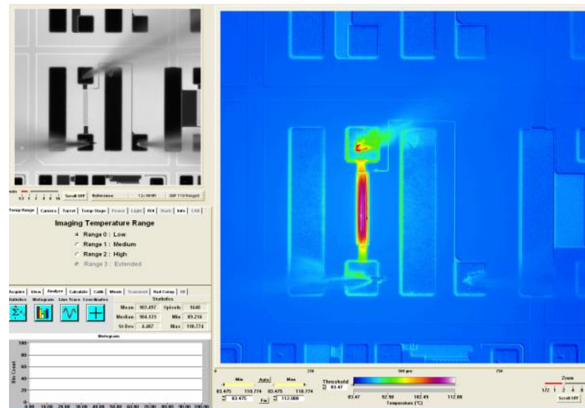

Fig 2: Device 1mm (Varying Ugw)

Device (mm)	Voltage (V)	Power (W)	Temp measured Value (^{0}C)
0.125	1	0.02	88.3
0.125	2	0.052	95.7
0.125	3	0.069	103.2
0.25	1	0.03	89.45
0.25	2	0.084	97.6
0.25	3	0.108	107.8
0.375	1	0.04	89.49
0.375	2	0.116	103.22
0.375	3	0.144	110.07
0.5	1	0.055	90.184
0.5	2	0.14	104.79
0.5	3	0.18	114.63
1	1	0.1	90.85
1	2	0.4	110.77
1	3	0.54	127.61

TABLE III: Measured Temperature
(Devices with Varying Ugw)

IJERT

III. ANALYTICAL APPROACH

A rectangular heat source is located at some depth z', with corners of heat source are at (x1,y1,z'),(x2,y1,z'),(x1,y2,z') and (x2,y2,z'). The elemental temperature increase (T) at point source (x,y,z) is given as [14]:

(This work is licensed under a Creative Commons Attribution 4.0 International License.)

$$T = \frac{Q_T}{4.\pi.k.r} dx' dy' \qquad (a)$$

$$r = \sqrt{(x-x')^2 + (y-y')^2 + (z-z_s)^2}$$

Where r is the distance between the heat source and the temperature distribution in the infinite medium at (x,y,z). The temperature distribution T(r) is obtained by integrating equation (a) where Q_T is power per unit area

$$T(r) = \int_{x_1}^{x_2}\int_{y_1}^{y_2} \frac{Q_T}{4.\pi.k.r} \qquad (b)$$

$$T(r) = \frac{Q_T}{4.\pi.k} \int_{\delta x_1}^{\delta x_2}\int_{\delta y_1}^{\delta y_2} \frac{d(\delta x)d(\delta y)}{\sqrt{\delta x^2 + \delta y^2 + \delta z^2}} \qquad (c)$$

Where δx = x - x', δy = y - y', δz = z – z', δx1 = x – x1, δy1 = y – y1, δx2 = x – x2, δy2 = y – y2Integrating equation (c) with respect to δy

$$T(r) = \frac{Q_T}{4.\pi.k} \int_{\delta y_1}^{\delta y_2} \frac{d(\delta y)}{\sqrt{\delta x^2 + \delta y^2 + \delta z^2}}$$

$$T(r) = \frac{Q_T}{4.\pi.k} \left[\log\left(\delta y + \sqrt{\delta x^2 + \delta y^2 + \delta z^2}\right)\right]_{\delta y_1}^{\delta y_2} \qquad (d)$$

Now integrating equation d with respect to δx i.e without solving for the limit for previous relation [14].

$$T(r) = \frac{Q_T}{4.\pi.k} \int_{\delta x_1}^{\delta x_2} \left[\log\left(\delta y + \sqrt{\delta x^2 + \delta y^2 + \delta z^2}\right)\right] d(\delta x)$$

$$T(r) = \frac{Q_T}{4.\pi.k} \left[(a + b)_{\delta y_1}^{\delta y_2}\right]_{\delta x_1}^{\delta x_2}$$

$$a(\delta x, \delta z) = \delta z \tan^{-1}\frac{\delta x}{\delta z} - \delta x$$

$$b(\delta x, \delta y, \delta z) = \delta x \log\left(\delta y + \sqrt{\delta x^2 + \delta y^2 + \delta z^2}\right) + \delta y \log\left(\delta x + \sqrt{\delta x^2 + \delta y^2 + \delta z^2}\right) - \delta z \tan^{-1}\left(\frac{\delta x \delta y}{\delta z \sqrt{\delta x^2 + \delta y^2 + \delta z^2}}\right)$$

From above equation we can see that term 'a' does not have any δy dependency so the whole term 'a' can be neglected and we are left with only term 'b'. Therefore the temperature distribution after integral value is given as

$$T(r) = \frac{Q_T}{4.\pi.k}\left[\begin{array}{l} b(\delta x_2, \delta y_2, \delta z) + b(\delta x_1, \delta y_1, \delta z) \\ - b(\delta x_1, \delta y_2, \delta z) - b(\delta x_2, \delta y_1, \delta z) \end{array}\right]$$

Where Q_T is the power density per unit area, k is the thermal conductivity. Where Q_T is P / WL.

To check the temperature increase distribution for each device at the end of the substrate, we need to incorporate the boundary conditions [14] equation (e) for upper and (f) for bottom surface of the substrate.

$$\left.\frac{\partial T(r)}{\partial z}\right|_{z=0} = 0 \qquad (e)$$

$$T(r)(x, y, z = d) = 0 \qquad (f)$$

With the help of method of images [14] shown in the figure3

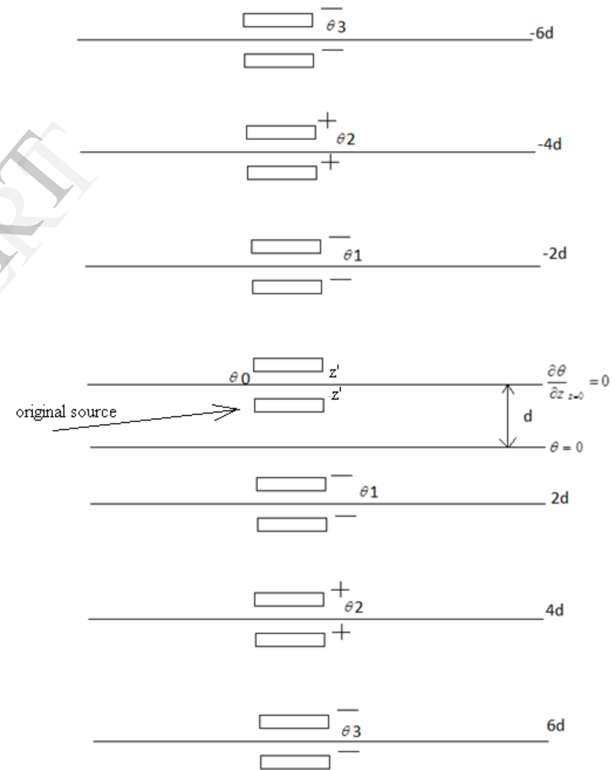

Fig3: Method of Images for determining the temp distribution

The original heat source is located at some depth z', the mirror image is located the same z' depth above the center line, which implies one is at + direction and the other one is at negative direction. In this study with the figure below, all the heat sources above the center line are negative distances, whereas the heat sources located below the center line are positive distances. The overall heat source addition at the center is names as θ0 which is the addition of both the sources to obtain the boundary condition to be satisfied at the

(This work is licensed under a Creative Commons Attribution 4.0 International License.)

top surface. In order to satisfy the boundary condition at z = d where the temperature distribution tends to zero, 2 heat sources are added at distance 2d. The 2 heat sources (θ1) located at distance 2d are negative heat sources so that they cancel with the heat sources located at center, to get the temperature increase zero at distance d i.e. (θ = 0 in figure). As a result of this the second boundary condition is satisfied, but due to this the first boundary condition is not satisfied. In order to satisfy the first boundary condition, we need to add two same negative heat sources at negative distance through mirror image. This procedure continues and is infinite long to satisfy both the conditions. Experiment was tried to carry out for varying n i.e. number of heat sources located at different distances. With n (no of heat sources) = 100 we can see it is as close to as zero at the bottom surface at z' =d shown in the figures below. The temperature increase distribution shown is for horizontal axis i.e along the x axis in the infinite medium.

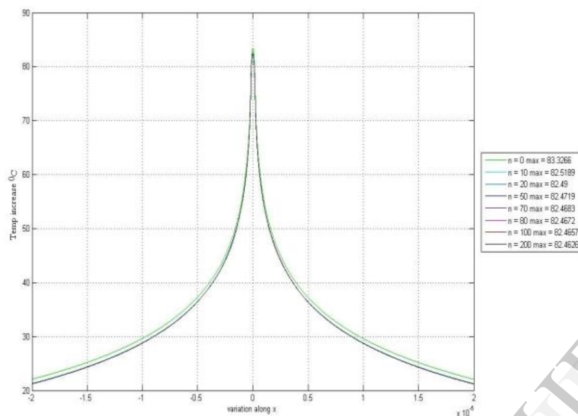

Fig 4: varying n, z'=0.01*10-6

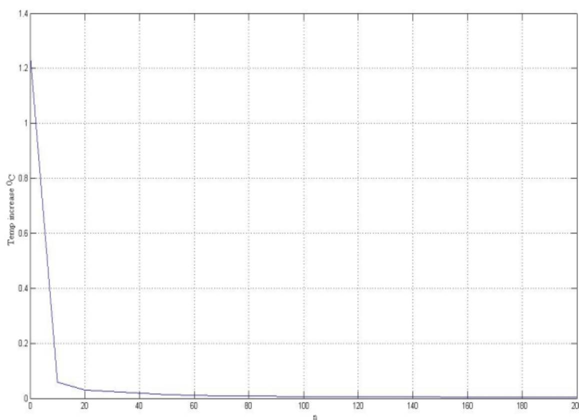

Fig 5: varying n, z'=d=635*10^-6

n	temp increase at bottom surface
0	1.2492
10	0.059611
20	0.030532
50	0.012394
70	0.0088782
80	0.0077753
100	0.006228
200	0.0031218

Table IV: temperature increase with varying n

IV. MULTI DEVICE OPTIMIZATION

A number of DC I-V has been proposed for modeling of GaAs Mesfets [10]-[12]. Figure 6 shows the equivalent circuit of HEMT used in this study. Modified Angelov model has been used to predict the dc behavior [13]

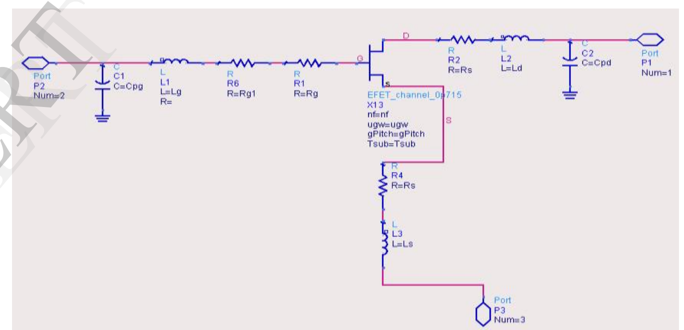

Fig 6: Equivalent circuit model for HEMT

The five-diode models each with varying nf and ugw are then extracted simultaneously by performing a multi-device optimization. Tentative scaling rules with unknown coefficients are assumed for each size-dependent model parameter. The model parameters can then be represented with the scaling rules, and the same model parameters for different devices are thus correlated. Instead of the model parameters, the unknown coefficients inside the scaling rules are now defined as the optimal variables. The error function now is the sum of the difference between the measurement and simulation for all of the devices. Multi device optimizations were carried out for all the devices with varying Nf and varying Ugw i.e each of them had five sets of devices. Each of the devices had around 39 parameters, so there were five times parameters for each multi device simulations. The thermal resistance value was compared to value obtained from the experimental measurement of each device. The optimization technique used for multi-device optimization in this study is the random and gradient optimization. Study started with random optimization to have the initial values for fitting, and after that gradient optimization type has been used.

(This work is licensed under a Creative Commons Attribution 4.0 International License.)

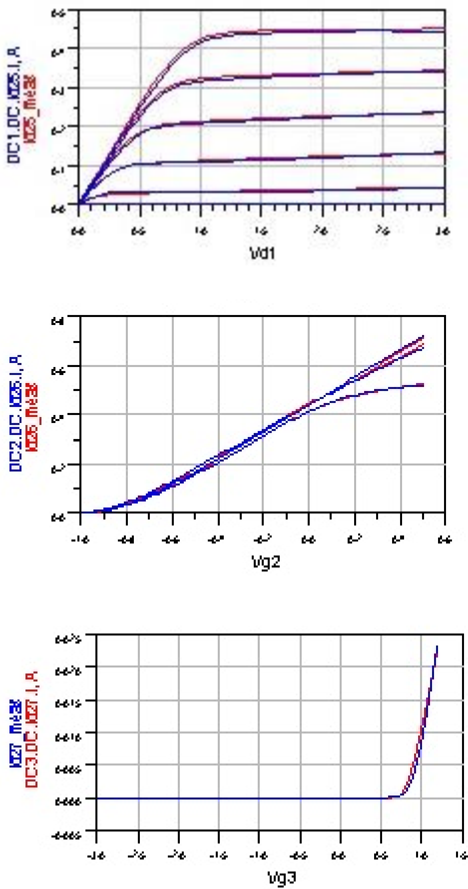

Fig 7: Output, transfer and Ig-Vg characteristics for Gate Width 3.4mm (Multi Device Optimization varying Nf)

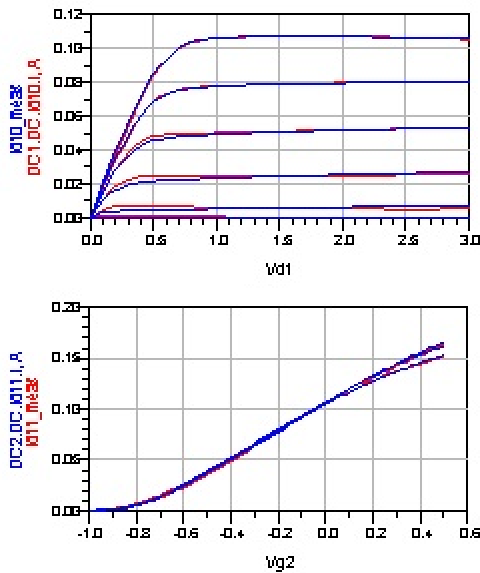

Fig 8: Output, transfer and Ig-Vg characteristics for Gate Width 0.5mm (Multi Device Optimization varying Ugw)

As shown in Figs 7 and 8, excellent matches between the measurement and simulation have been achieved for output, transfer and Ig-Vg characteristics. The blue line is the measured data and the red one is the simulated result.

Gate Width (mm)	α	γ	Rth (ohms)	Rs(ohms)	Rg (ohms)
0.125	0.70	2.99	302.24	4.94	11.21
0.25	0.70	2.99	195.01	2.78	11.32
0.375	0.70	2.99	153.62	2.07	11.43
0.5	0.70	2.99	126.01	1.71	11.55
1	0.70	2.99	72.32	1.17	12

TABLE V: Parameters extracted with multi device optimization with varying Ugw

Gate Width (mm)	α	γ	Rth (ohms)	Rs(ohms)	Rg (Ohms)
0.715	0.70	2.48	100.85	1.38	11.74
1	0.70	2.48	82.51	1.17	12
2	0.70	2.48	59.5	0.90	12.9
3	0.70	2.48	51.83	0.81	13.8
3.4	0.70	2.48	50.03	0.79	14.16

TABLE VI: Parameters extracted with multi device optimization with varying Nf

Some extracted parameters from multi-device optimization are shown in Table V and VI. The size dependent parameter follows exactly the scaling rule, and the size independent parameter keep the same value for different devices.

IJERT

(This work is licensed under a Creative Commons Attribution 4.0 International License.)

V. RESULTS

The equation derived for temperature distribution is used to find the temperature distribution profile for all the devices at different voltages with varying Nf and Ugw. The heat source position as described earlier in the equation are used as the length and unit gate width parameters to define the value along with variable to define to Nf in Matlab. The values for x1, x2, y1, y2 and z' are -0.2µm, 0.2µm, -71.5µm, 71.5µm and 0.01µm to keep all the parameters of the same unit, so that the length of the device is 0.4µm which is fixed and Ugw is 143µm which is dependable on the device Ugw size.

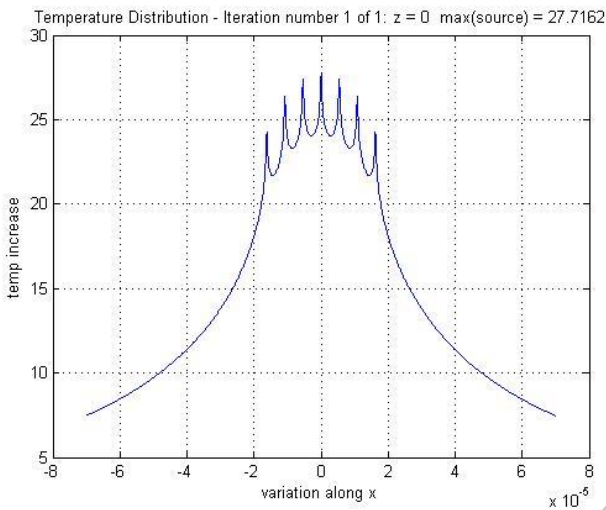

Fig 9: Temp distribution of device 1mm with Nf = 7 and Ugw = 143 at 2V.

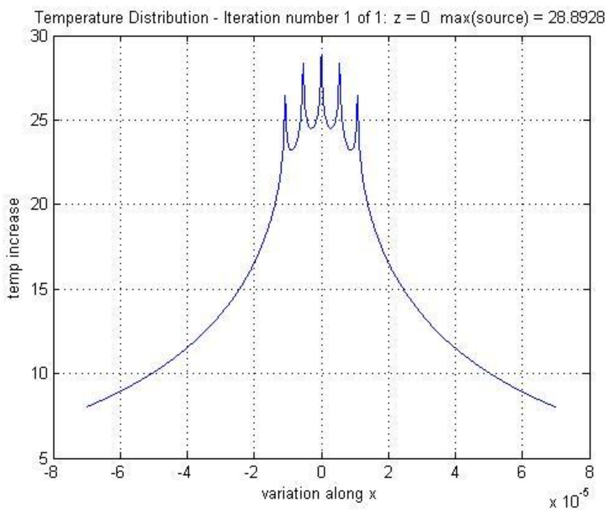

Fig 10: Temp distribution of device 1mm with Nf = 5 and Ugw = 200 at 2V.

Table's VII and VIII show the values of each device at different voltage. Power is calculated by the simple V*I, where current for each device is recorded while performing the experiment. The analytical value extracted for each device at each voltage by varying Nf and Ugw is recorded. To the analytical value reference value of 85^0C is added in order to compare the values obtained with that of experiment, as the reference plate was at 85^0C while measuring the temperature behavior of each device. Main concentration was in the linear region of the device till 2 V.

TABLE VII: Comparison between analytical and measured Temp value for devices with Varying Nf

Device (mm)	Voltage (V)	Power (W)	Analytical value (^{0}C)	RefTemp +85^0C	Measured value (^{0}C)
0.715	1	0.1	9.2949	94.2989	89.8
0.715	2	0.28	26.0258	111.0258	97.3
0.715	3	0.36	33.4617	118.4617	127
1	1	0.12	9.7822	94.7822	90.16
1	2	0.34	27.7162	112.7162	112.3
1	3	0.45	36.6832	121.6832	133.1
2	1	0.15	9.1398	94.1398	91.5
2	2	0.48	29.2473	114.2473	114.1
2	3	0.69	42.043	127.043	152.4
3	1	0.19	9.5752	94.5752	92.45
3	2	0.72	36.2851	121.2851	120.8
3	3	1.02	51.4039	136.4039	176.1
3.4	1	0.23	10.8346	95.8346	95.89
3.4	2	0.86	40.5119	125.5119	126.8
3.4	3	1.23	57.9414	142.9414	184.3

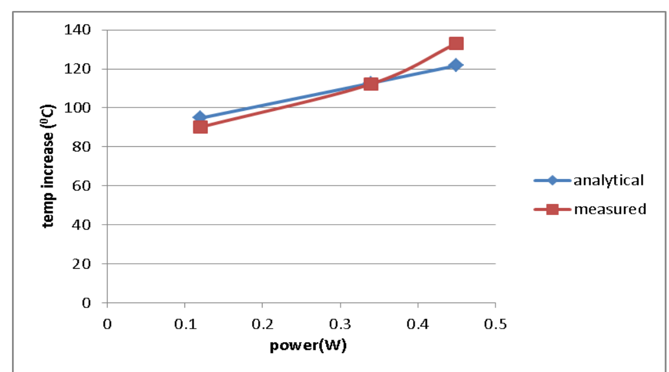

Fig 11: Analytical vs Measured for 1mm device (varying Nf)

IJERT

(This work is licensed under a Creative Commons Attribution 4.0 International License.)

Device (mm)	Voltage (V)	Power (W)	Analytical value (^{0}C)	Ref-Temp+85^{0}C	Measured value (^{0}C)
0.125	1	0.02	6.0169	91.0169	88.3
0.125	2	0.052	15.6439	100.643	95.7
0.125	3	0.069	20.7583	105.758	103.2
0.25	1	0.03	5.8359	90.8359	89.45
0.25	2	0.084	16.3404	101.340	97.6
0.25	3	0.108	21.0091	106.009	107.8
0.375	1	0.04	5.9128	90.9128	89.49
0.375	2	0.116	17.147	102.147	103.22
0.375	3	0.144	21.286	106.286	110.07
0.5	1	0.055	6.6361	91.6361	90.184
0.5	2	0.14	16.8919	101.891	104.79
0.5	3	0.18	21.7182	106.718	114.63
1	1	0.1	7.2232	92.2232	90.85
1	2	0.4	28.8928	113.892	110.77
1	3	0.54	39.0053	124.005	127.61

TABLE VIII: Comparison between analytical and measured Temp value for devices with Varying Ugw

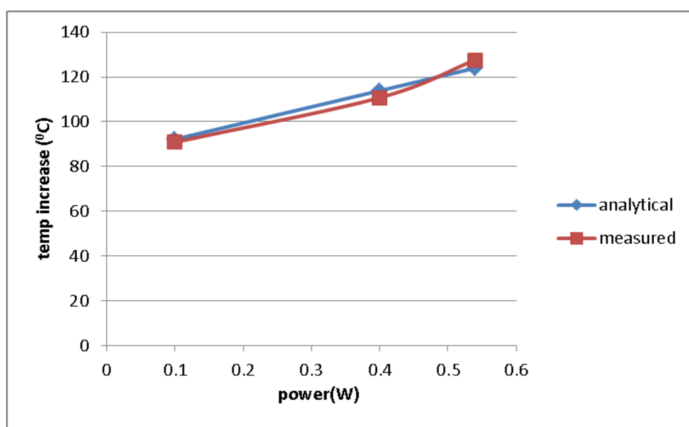

Fig 12: Analytical vs Measured for 1mm device (varying Ugw)

The thermal resistance is calculated with the power calculated for each device and is given as

P= V * I

Rth = ΔT / P

ΔT = T – room temp

Device (mm)	Rth (ohms)
0.125	300.5
0.25	194.3
0.375	147.7
0.5	120.6
1	72.7

TABLE IX: Rth Analytical Value (Varying Ugw)

Device (mm)	Rth (ohms)
0.715	92.7
1	81.5
2	60.8
3	50.3
3.4	47.1

TABLE X: Rth Analytical Value (Varying Nf)

Comparing the values of thermal resistance from the table V and VI obtained with the simulating data for devices on ADS with the analytical values from table IX and X, one can see that the value obtained are close enough and the fitting for output, transfer characteristics of each device are close to each as shown in figure’s 7 and 8.

The scaling rule of thermal resistance proposed in [14]-[16] are used in the study.

$$Rth = \frac{t}{kWL} \tag{7}$$

Where t is substrate thickness, k is the thermal conductivity, W is gate width, and L is the length. The extracted gate width dependence of Rth is shown in Fig 13 and 14. For the devices with self-heating effect, the accurate dc performance prediction cannot be achieved without an accurate scalable thermal resistance.

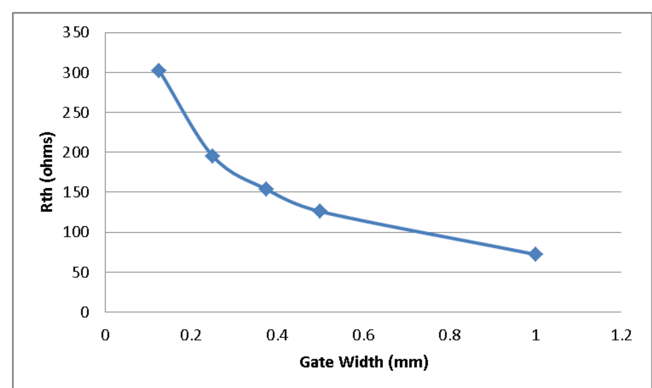

Fig13: Gate width vs. Rth (multi-device optimization Varying Ugw)

IJERT

(This work is licensed under a Creative Commons Attribution 4.0 International License.)

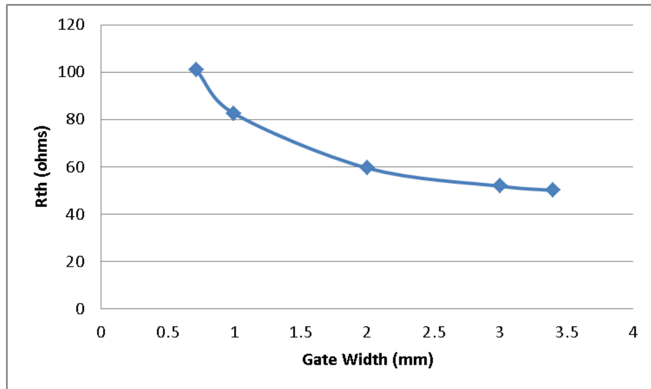

Fig14: Gate width vs. Rth (multi-device optimization Varying Nf)

CONCLUSION

A novel approach to extract dc HEMT model has been proposed and demonstrated with accurate extraction of thermal resistance. The experimental data compared to the analytical data for accurate values of thermal resistance is observed to be very close. The temperature distribution (horizontally or vertically) along with the maximum temperature across the fingers in each devices observed analytically vs experimentally has been very close. Scaling rule for thermal resistance has been confirmed for both the sets of devices with varying Nf and Ugw.

REFERENCES

[1] B. Castagnola, A. Giorgio, A.G. Perry,"Modeling Thermal effects on MESFET I-V characteristics" IEEE Electrotechnical Conference, Vol3, pp1298-1301, May 1996.

[2] Ingo Schmale, Gunter Kompa, "A novel thermal resistance technique for temperature-dependent FET modeling" GAAS, Amsterdam 1998.

[3]Anholt Robert "Electrical and Thermal Characteristics of MESFETs, HEMTs and HBTs" 1949.

[4] L. G. Walshak and W. E. Poole, "Thermal resistance measurement by IR scanning," Microwave J., vol. 16, pp. 62-65, Feb. 1977.

[5] B. S. Siegal, "A proposed method for testing thermal resistance of MESFETs," Microwave Syst. News, vol. 7, pp. 67-69, Nov. 1977.

[6] H. Fukui, "Thermal resistance of GaAs field-effect transistors," in IEDM Tech. Dig. (Washington, DC), pp. 118-121, 1980.

[7] A.H.Peake, C.G. Rogers and P.M. White," Improved thermal resistance procedure for GaAs FETs using pulsed electrical methode" in Proc Semiconductor Thermal and Temperature Measurement Symp., Dec 1984.

[8] C.E. Stephens and F.N.Sinnadurai,"A surface temperature limit detector using nematic liquid crystals with an application to microcircuits." J. physics E. Scientific Instr vol 7 pp 641-643, 1974.

[9] Donald B. Estreich," A DC Technique for Determining GaAs MESFET Thermal Resistance" IEEE Trans, vol 12 no 4 Dec 1989.

[10] W.R. Curtice, "A Mesfet Model for use in the design of GaAs Integrated circuits" IEEE Trans Microwave Theory, pp 448-56, May1980

[11] W.R. Curtice and M Ettenberg,"A Nonlinear GaAs FET model for use in the Design of output circuits for power amplifiers"IEEE Trans Microwave Theory tech, pp 1383-94, Dec 1985

[12] H.Statz, P Newman, I.W.Smith R.. A. Pucel, H.A.Haus,"GaAs Fet Device and Circuit Simulation in Spice"IEEE Trans Electron Devices vol ed 3, pp 160-69, Feb 1987.

[13] I. Angelov, H. Zirath, N. Rorsman, "A New Empirical NonLinear Model for HEMT and MESFET Devices," IEEE Transaction on Microwave Theory and Techniques, vol 40, no 12, pp 2258-2266, Dec 1992.

[14] N. Rinaldi,"Thermal analysis of solid-state devices and circuits an analytical approach." Solid-State Electronics, vol44, issue 10,pp 1789-1798, Oct 2000.

[15] Ali Mohamed, Andrew J. Bayba, H. Alfred Hung, "Accurate Determination of Thermal Resistance of FETs" Microwavetheory and Techniques, IEEE, vol 53 issue 1, pp 306-313, January 2005.

[16] A. Giorgio, A.G. Perri, B. Castagnolo, "Automatic design of GaAs MESFETs for thermal effect optimization" Gallium Arsenide Application Symposium, Paris CNAM, June 1996.

IJERT

(This work is licensed under a Creative Commons Attribution 4.0 International License.)